

Electronic Supplementary Information

Reducing Localized Over-aggregation and Non-radiative Energy Loss Enabled by a Nonacyclic Carbazole-Based Third Component for Over 18% Efficiency Polymer Solar Cells

*Yongshuai Gong,^a Runnan Yu,^a Huaizhi Gao,^a Zongwen Ma,^a Yiman Dong,^a Yi-Jia Su,^b Tsung-Wei Chen,^b Chain-Shu Hsu,^{*b} and Zhan'ao Tan^{*a}*

^a. Beijing Advanced Innovation Center for Soft Matter Science and Engineering, State Key Laboratory of Organic-Inorganic Composites, Beijing University of Chemical Technology Beijing 100029, China.

E-mail: tanzhanao@mail.buct.edu.cn

^b. Department of Applied Chemistry and Center for Emergent Functional Matter Science, National Yang Ming Chiao Tung University, 1001 University Road, Hsinchu 30010, Taiwan.

E-mail: cshsu@mail.nctu.edu.tw

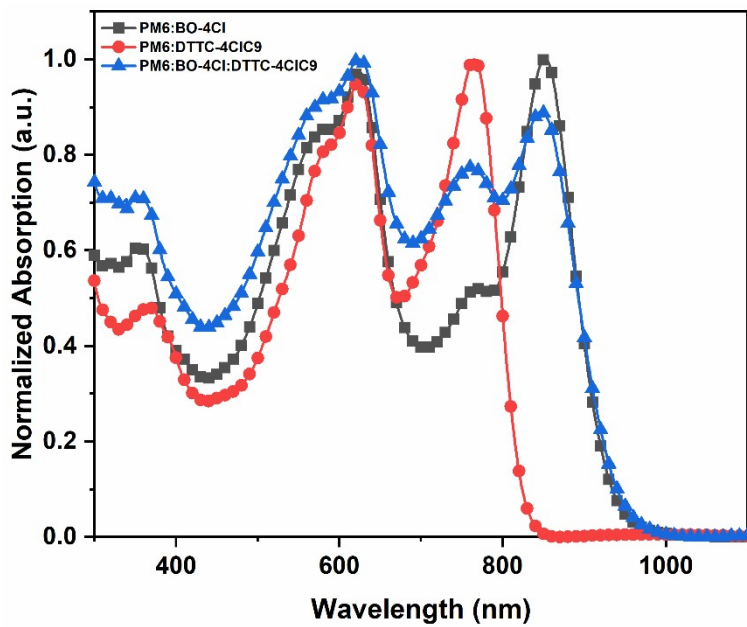


Fig. S1. UV-vis absorption of the binary and ternary blend films.

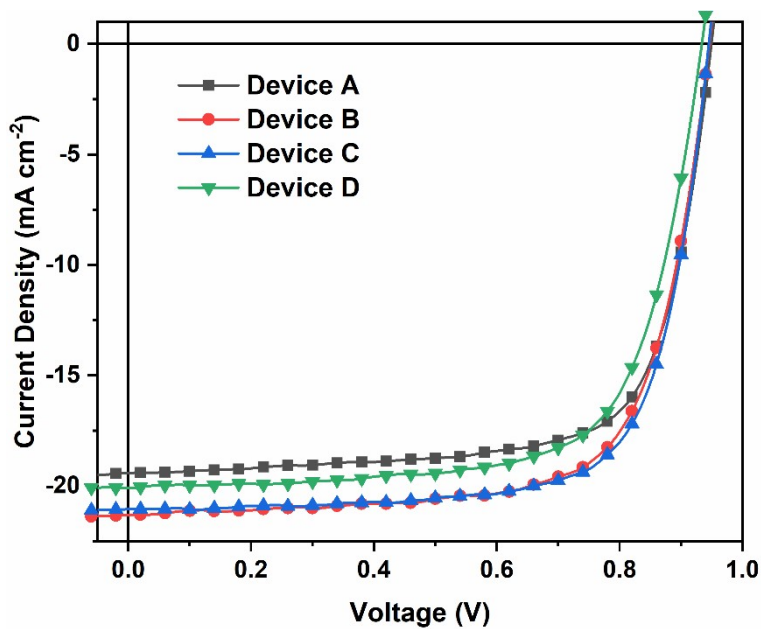


Fig. S2. Optimization of PM6:DTTC-4ClC9 based binary devices.

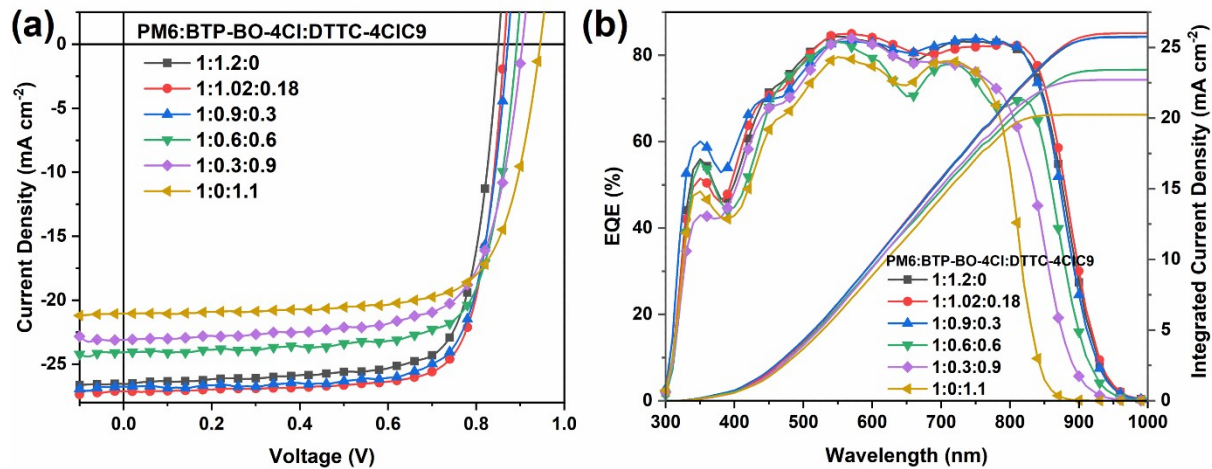


Fig. S3. (a) J - V curves and (b) EQE spectra of the PM6:BTP-BO-4Cl:DTCC-4ClC9 based devices with different ratio.

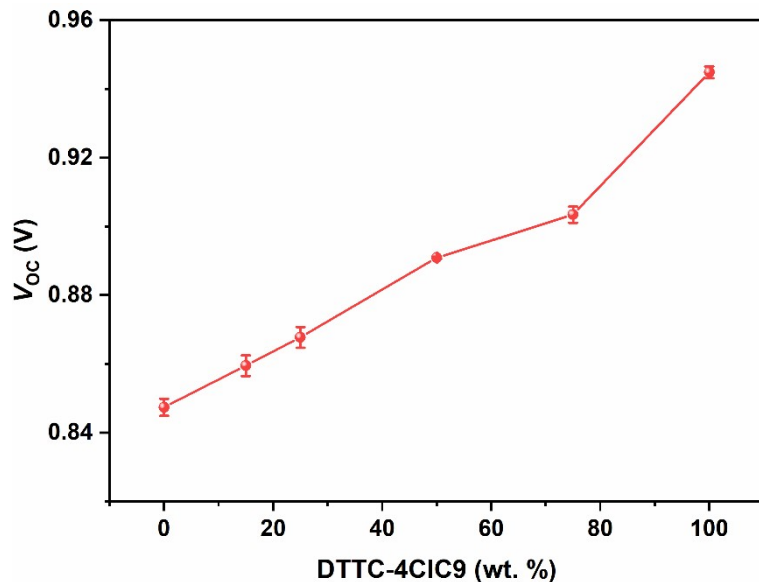
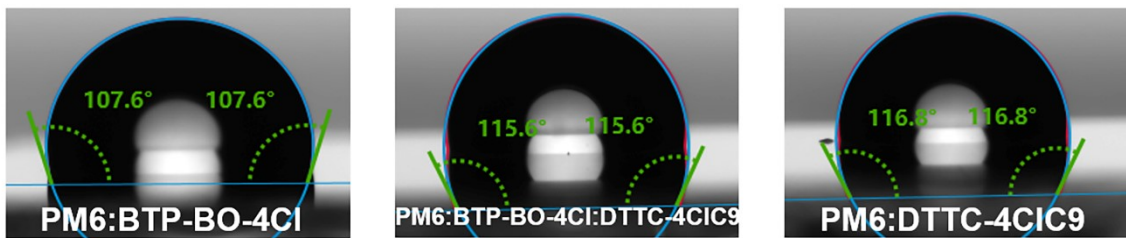


Fig. S4. The variation of V_{OC} of all devices with different DTTC-4ClC9 contents.

(a) WCA



(b) DCA



Fig. S5. (a) Water and (b) diiodomethane contact angle of PM6:BTP-BO-4Cl, PM6:BTP-BO-4Cl:DTTC-4ClC9, and PM6:DTTC-4ClC9 blend films.

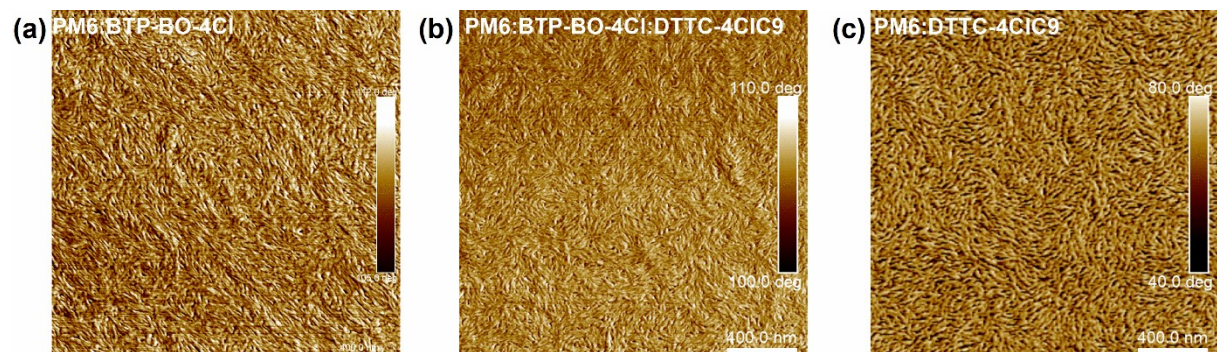


Fig. S6. AFM phase images of PM6:BTP-BO-4Cl, PM6:BTP-BO-4Cl:DTTC-4ClC9, and PM6:DTTC-4ClC9 blend films.

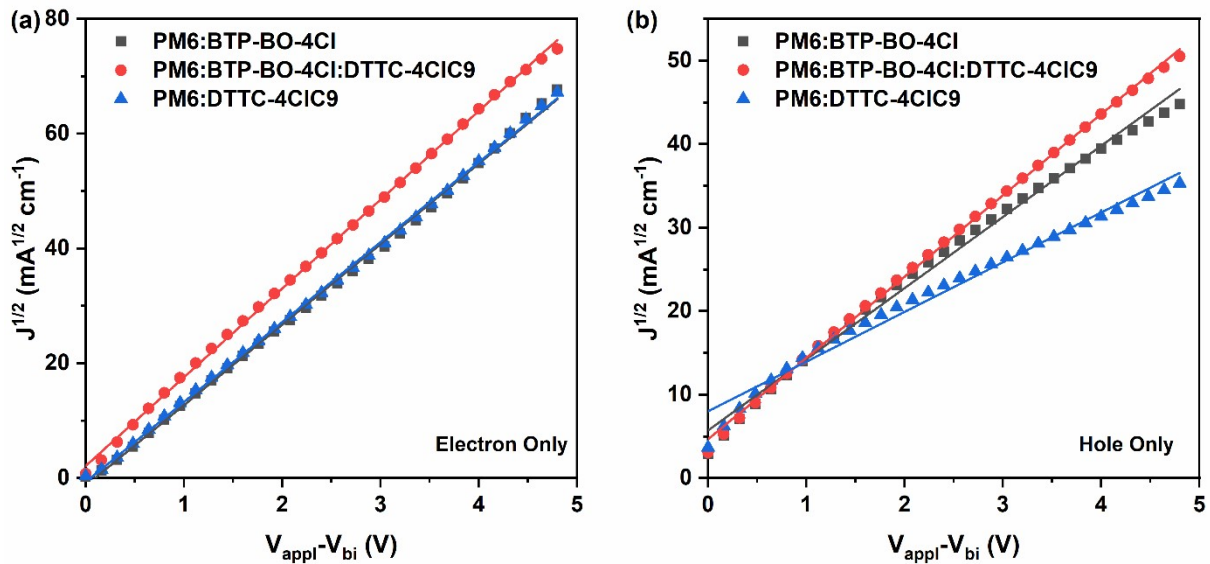


Fig. S7. (a) The electron and (b) hole mobility of PM6:BTP-BO-4Cl, PM6:BTP-BO-4Cl:DTTC-4ClC9 and PM6:DTTC-4ClC9 blend films measured by SCLC method.

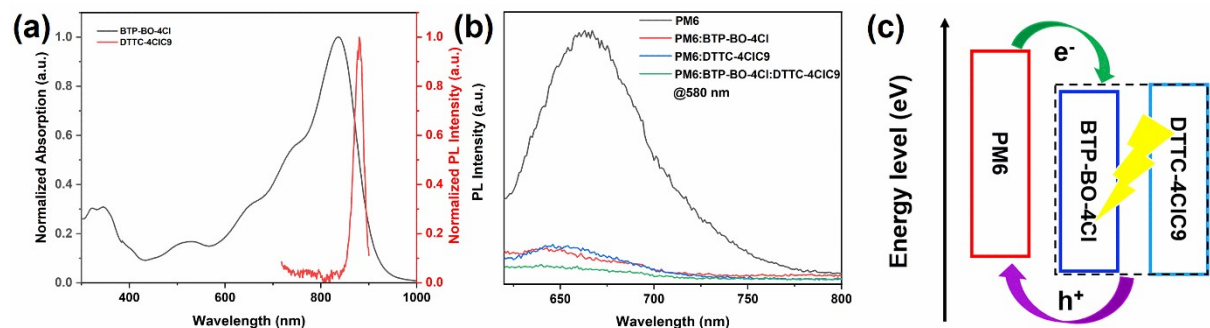


Fig. S8. (a) Normalized absorption spectrum of neat BTP-BO-4Cl film and normalized PL spectrum of neat DTTC-4ClC9 film, (b) PL spectra of PM6, PM6:BTP-BO-4Cl, PM6:BTP-BO-4Cl:DTTC-4ClC9, and PM6:DTTC-4ClC9 films excited at 580 nm, and (c) schematic of the charge transfer process in the ternary blend.

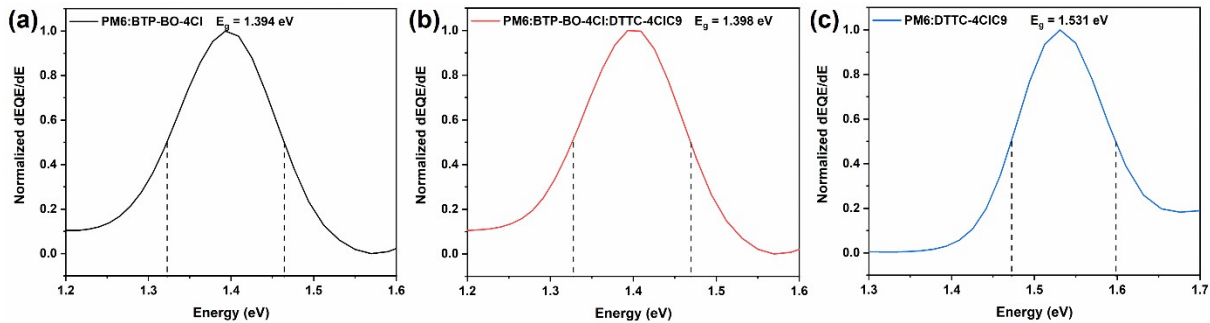


Fig. S9. Optical bandgap determination of (a) PM6:BTP-BO-4Cl, (b) PM6:BTP-BO-4Cl:DTTC-4ClC9, and (c) PM6:DTTC-4ClC9 blends. The region between dashed lines is the part where the gap distribution probability is greater than half of the maximum, which is used for the bandgap calculation.

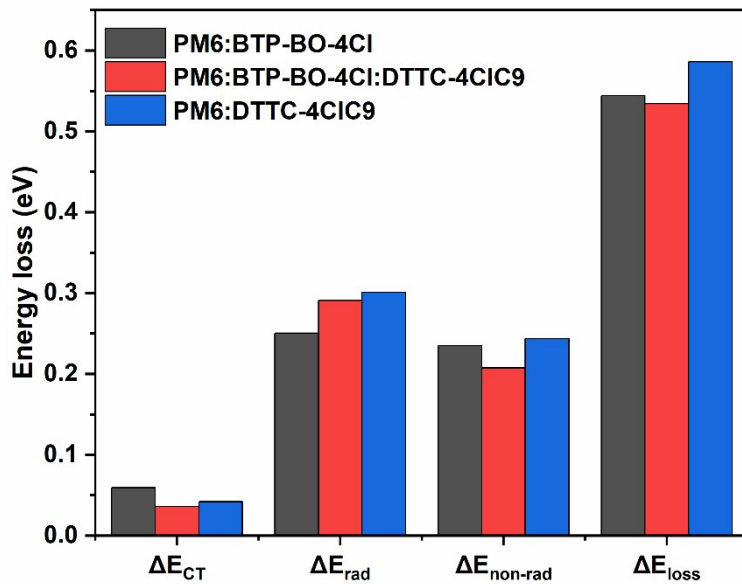


Fig. S10. Total energy loss (E_{loss}) and different contributions to E_{loss} in the binary and ternary solar cells.

Table S1. Summary of photovoltaic parameters of the PM6:DTCC-4ClC9 based binary devices fabricated under different conditions.

Ratio	V_{OC} [V]	J_{SC} [mA cm^{-2}]	FF [%]	Best PCE [%]
Device A	0.949	19.42	72.25	13.31
Device B	0.945	21.31	70.71	14.25
Device C	0.945	21.05	72.92	14.50
Device D	0.933	20.09	69.85	13.10

Fabrication condition:

Device A: Donor concentration (C_D) is 7 mg/mL, spin-coating speed is 3000 rpm.

Device B: C_D is 8 mg/mL, spin-coating speed is 3000 rpm.

Device C: C_D is 8 mg/mL, spin-coating speed is 4000 rpm.

Device D: C_D is 9 mg/mL, spin-coating speed is 4000 rpm, annealing 100 °C for 10 min.

Table S2. Summary of photovoltaic parameters of the PM6:BTP-BO-4Cl:DTCC-4ClC9 based devices with different ratio.

Ratio	V_{OC} [V]	J_{SC} [mA cm ⁻²]	$J_{SC}^a)$ [mA cm ⁻²]	FF [%]	PCE ^{b)} [%]
1:1.2	0.850	26.54	25.77	75.86	17.11 (16.90 ± 0.14)
1:0.02:0.18	0.864	27.12	26.01	77.76	18.21 (17.91 ± 0.15)
1:0.9:0.3	0.871	26.75	25.73	76.40	17.80 (17.27 ± 0.27)
1:0.6:0.6	0.891	24.06	23.42	75.27	16.14 (15.68 ± 0.29)
1:0.3:0.9	0.905	23.09	22.71	71.77	14.99 (14.60 ± 0.32)
1:1.1	0.945	21.05	20.24	72.92	14.50 (14.34 ± 0.13)

^{a)} Integrated J_{SC} calculated from EQE.

^{b)} Average values were obtained from over 10 individual devices.

Table S3. Surface energy characteristics of the PM6, BTP-BO-4Cl, DTCC-4ClC9, and BTP-BO-4Cl:DTTC-4ClC9 films and the related Flory–Huggins interaction parameters (χ).

Material	WCA (°)	DCA (°)	γ (mN m ⁻¹)	Blend	χ
PM6	104.1	50.2	36.21	PM6:BTP-BO-4Cl	0.25K
BTP-BO-4Cl	101.4	39.6	42.46	PM6:DTTC-4ClC9	1.13K
DTTC-4ClC9	107.2	36.8	50.02	BTP-BO-4Cl:DTTC-4ClC9	0.31K
BTP-BO-4Cl:DTTC-4ClC9	101.8	37.8	43.73	PM6:BTP-BO-4Cl:DTTC-4ClC9	0.35K

Table S4. Surface energy characteristics of the PM6:BTP-BO-4Cl, PM6:BTP-BO-4Cl:DTTC-4ClC9, and PM6:DTTC-4ClC9 blend films.

Blend film	WCA (°)	DCA (°)	γ (mN m ⁻¹)
PM6:BTP-BO-4Cl	107.6	50.3	37.25
PM6:BTP-BO-4Cl: DTTC-4ClC9	115.6	49.7	41.12
PM6:DTTC-4ClC9	116.8	55.7	36.77

Table S5. Crystal coherence lengths of the (010) peak and the d-spacing for the blend films.

Active Layer	q (Å⁻¹)	d-spacing (Å)	FWHM (Å⁻¹)	CCL (nm)
PM6:BTP-BO-4Cl	1.725	3.64	0.3911	1.61
PM6:BTP-BO-4Cl:DTTC-4ClC9	1.741	3.61	0.3867	1.63
PM6:DTTC-4ClC9	1.703	3.69	0.4978	1.26

Table S6. Crystal coherence lengths of the (100) peak and the d-spacing for the blend films.

Active Layer	q (Å⁻¹)	d-spacing (Å)	FWHM (Å⁻¹)	CCL (nm)
PM6:BTP-BO-4Cl	0.297	21.16	0.1046	6.01
PM6:BTP-BO-4Cl:DTTC-4ClC9	0.297	21.16	0.0986	6.37
PM6:DTTC-4ClC9	0.273	23.02	0.0868	7.24

Table S7. Summary of photovoltaic parameters of the recent reported ternary PSCs.

Host blend	Third component	V_{OC} [V]	J_{SC} [mA cm⁻²]	FF [%]	Best PCE [%]	Ref.
PM6:Y6	IDTT-M ^{a)}	0.872	25.81	73.89	16.63	1
PM6:Y6	3TP3T-4F ^{a)}	0.85 ± 0.01	25.9 ± 0.3	74.9 ± 1.0	16.7	2
PM6:Y6	IDTP-4F ^{a)}	0.863	25.7	77.2	17.1	3
PM6:Y6	MOITIC ^{a)}	0.882	25.6	75.7	17.1	4
PM6:BTP-4F-12	IT-M ^{a)}	0.875	25.95	78.02	17.71	5
PBQx-TF:eC9-2Cl	F-BTA3 ^{a)}	0.879	26.7	80.9	19.0	6
PM6:BTP-ClBr1	BTP-2O-4Cl-C12 ^{b)}	0.891	25.45	75.8	17.19	7
PM6:Y6	BTIC-EH-2ThBr ^{b)}	0.853	26.39	77.90	17.54	8
PM6:Y6	AQx-3 ^{b)}	0.870	26.82	77.2	18.01	9

Host blend	Third component	V_{OC} [V]	J_{SC} [mA cm $^{-2}$]	FF [%]	Best PCE [%]	Ref.
PM6:BO-4Cl	BTP-S2 ^{b), c)}	0.861	27.14	78.04	18.16	¹⁰
PM6:BTP-eC9	BTP-F ^{b)}	0.858	26.99	79.7	18.45	¹¹
PM6:Y6	TPD-3F ^{d)}	0.88 ± 0.01	25.6 ± 0.18	73.4 ± 0.90	17.0	¹²
PM6:Y6	DRTB-T-C4 ^{d)}	0.854	24.68	80.88	17.05	¹³
PM6:Y6	DRTB-T-C4 ^{d)}	0.85	24.79	81.3	17.13	¹⁴
PM7:Y7	SiCl-BDT ^{d)}	0.86 ± 0.02	27.73 ± 0.32	70.43 ± 3.0	17.40	¹⁵
PM6:Y6	S3 ^{d)}	0.856	25.86	79.17	17.53	¹⁶
PM6:Y6	BTTzR ^{d)}	0.87	26.2	77.7	17.7	¹⁷
PM6:BTP-eC9	BPR-SCl ^{d)}	0.856	27.13	0.776	18.02	¹⁸
PM6:BTP-eC9	PB2F ^{d)}	0.863	26.8	80.4	18.6	¹⁹
PM6:BTP-BO-4Cl	BTP-T-3Cl ^{b)}	0.857	27.38	77.73	18.21	²⁰
PM6:BTP-BO-4Cl	DTTC-4ClC9	0.864	27.12	77.76	18.21	This work

^{a)} ITIC derivatives; ^{b)} BTP-series acceptors; ^{c)} layer-by-layer device; ^{d)} a second donor.

References

1. L. G. Xiao, X. Wu, G. X. Ren, M. A. Kolaczkowski, G. Huang, W. Y. Tan, L. Ma, Y. D. Liu, X. B. Peng, Y. G. Min and Y. Liu, *Adv. Funct. Mater.*, 2021, **31**, 2105304.
2. J. L. Song, C. Li, L. Zhu, J. Guo, J. Q. Xu, X. N. Zhang, K. K. Weng, K. N. Zhang, J. Min, X. T. Hao, Y. Zhang, F. Liu and Y. M. Sun, *Adv. Mater.*, 2019, **31**, 1905645.
3. J. Hu, Q. Guo, J. Fang, Q. Liu, H. Liang, J. Lv, Z. Yin, J. Lin, X. Ou, X. Guo and M. Zhang, *Org. Electron.*, 2021, **95**, 106201.
4. M. Xiong, J. Wu, Q. Fan, Q. Liu, J. Lv, X. Ou, X. Guo and M. Zhang, *Org. Electron.*, 2021, **96**, 106227.
5. J. Gao, X. Ma, C. Xu, X. Wang, J. H. Son, S. Y. Jeong, Y. Zhang, C. Zhang, K. Wang, L. Niu, J. Zhang, H. Y. Woo, J. Zhang and F. Zhang, *Chem. Eng. J.*, 2022, **428**, 129276.
6. Y. Cui, Y. Xu, H. Yao, P. Bi, L. Hong, J. Zhang, Y. Zu, T. Zhang, J. Qin, J. Ren, Z. Chen, C. He, X. Hao, Z. Wei and J. Hou, *Adv. Mater.*, 2021, **33**, 2102420.
7. R. Ma, Y. Tao, Y. Chen, T. Liu, Z. Luo, Y. Guo, Y. Xiao, J. Fang, G. Zhang, X. Li, X. Guo, Y. Yi, M. Zhang, X. Lu, Y. Li and H. Yan, *Sci. China Chem.*, 2021, **64**, 581-589.
8. C. C. Cao, H. J. Lai, H. Chen, Y. L. Zhu, M. R. Pu, N. Zheng and F. He, *J. Mater. Chem. A*, 2021, **9**, 16418-16426.
9. F. Liu, L. Zhou, W. R. Liu, Z. C. Zhou, Q. H. Yue, W. Y. Zheng, R. Sun, W. Y. Liu, S. J. Xu, H. J. Fan, L. H. Feng, Y. P. Yi, W. K. Zhang and X. Z. Zhu, *Adv. Mater.*, 2021, **33**, 2100830.
10. L. Zhan, S. Li, X. Xia, Y. Li, X. Lu, L. Zuo, M. Shi and H. Chen, *Adv. Mater.*, 2021, **12**, 2007231.
11. Y. Li, Y. H. Cai, Y. P. Xie, J. H. Song, H. B. Wu, Z. Tang, J. Zhang, F. Huang and Y. M. Sun, *Energ. Environ. Sci.*, 2021, **14**, 5009-5016.

12. B. H. Jiang, Y. P. Wang, C. Y. Liao, Y. M. Chang, Y. W. Su, R. J. Jeng and C. P. Chen, *Acs Appl. Mater. Inter.*, 2021, **13**, 1076-1085.
13. Y. Zeng, D. Li, Z. Xiao, H. Wu, Z. Chen, T. Hao, S. Xiong, Z. Ma, H. Zhu, L. Ding and Q. Bao, *Adv. Energy. Mater.*, 2021, **11**, 2101338.
14. D. Q. Li, L. Zhu, X. J. Liu, W. Xiao, J. M. Yang, R. R. Ma, L. M. Ding, F. Liu, C. G. Duan, M. Fahlman and Q. Y. Bao, *Adv. Mater.*, 2020, **32**, 2002344.
15. T. Gokulnath, J. Choi, H.-Y. Park, K. Sung, Y. Do, H. Park, J. Kim, S. S. Reddy, J. Kim, M. Song, J. Yoon and S.-H. Jin, *Nano Energy*, 2021, **89**, 106323.
16. Q. An, J. Wang, X. Ma, J. Gao, Z. Hu, B. Liu, H. Sun, X. Guo, X. Zhang and F. Zhang, *Energ. Environ. Sci.*, 2020, **13**, 5039-5047.
17. Q. Liu, Y. Wang, J. Fang, H. Liu, L. Zhu, X. Guo, M. Gao, Z. Tang, L. Ye, F. Liu, M. Zhang and Y. Li, *Nano Energy*, 2021, **85**, 105963.
18. X. Chen, D. Wang, Z. Wang, Y. Li, H. Zhu, X. Lu, W. Chen, H. Qiu and Q. Zhang, *Chem. Eng. J.*, 2021, **424**, 130397.
19. T. Zhang, C. An, P. Bi, Q. Lv, J. Qin, L. Hong, Y. Cui, S. Zhang and J. Hou, *Adv. Energy. Mater.*, 2021, **n/a**, 2101705.
20. Y. Pan, X. Zheng, J. Guo, Z. Chen, S. Li, C. He, S. Ye, X. Xia, S. Wang, X. Lu, H. Zhu, J. Min, L. Zuo, M. Shi and H. Chen, *Adv. Funct. Mater.*, 2021, DOI: 10.1002/adfm.202108614, 2108614.